$^{15}N-^{1}H$ HSQC NMR Evidence for Distinct Specificity of Two Active Sites in *Escherichia coli* Glyoxalase I[†]

Zhengding Su,[‡] Nicole Sukdeo,[‡] and John F. Honek*

Department of Chemistry, University of Waterloo, Waterloo ON N2L 3G1, Canada

Received July 14, 2008; Revised Manuscript Received October 16, 2008

ABSTRACT: Much remains to be elucidated concerning the selectivity mechanism of supposedly identical active sites in oligomeric proteins. Glyoxalase I (GlxI) catalyzes the glutathione-dependent conversion of 2-oxoaldehydes to *S*-2-hydroxyacylglutathione derivatives. The *E. coli* GlxI is a Ni^{2+}/Co^{2+}-activated homodimeric protein containing two symmetric, and dually metallated active sites as characterized by X-ray structure determination. Nevertheless, kinetics and isothermal titration calorimetric (ITC) studies indicate that dimeric GlxI binds to metal ions in a ratio of 1:1 (one metal ion/one dimer) [Clugston, S. L., Yajima, R., and Honek, J. F. (2004) *Biochem. J. 377*, 309−316]. In the current study, we provide spectroscopic evidence for the nonequivalent metallation of GlxI by use of $^{15}N-^{1}H$ HSQC NMR titration experiments. $^{15}N-^{1}H$ HSQC NMR spectra reveal that the local conformations of the two active sites in homodimeric GlxI are initially asymmetric in the apo-form, resulting in functional differentiation, wherein only one active site binds to the Ni^{2+} ion, and another active site is observed to be more selective for a potent inhibitor. The current results enhance our understanding of GlxI structure−function relationships and provide a potential new strategy for the development of small molecule inhibitors for this enzyme system.

Glyoxalase I (GlxI[1]), a member of the metalloglutathione transferase superfamily, catalyzes the first step of the detoxification of cytotoxic methyglyoxal (MG) via the conversion of nonenzymatically produced HG-GSH hemithioacetals to *S*-D-lactoylglutathione (Figure 1a) and thereby plays a critical detoxification role in cells (*1*−*3*). GlxI is also a key component in the prevention of glycation reactions mediated by methylglyoxal, glyoxal and other α-oxoaldehydes *in vivo* (*2*). The glyoxalase system in mammals has complex kinetics, which have been analyzed by ^{1}H NMR and modeling (*4*). Inhibition of GlxI pharmacologically with specific inhibitors leads to the accumulation of alpha-oxoaldehydes to cytotoxic levels. Cell-permeable GlxI inhibitors have been found to be potent antimalarial agents against *Plasmodium falciparum*, an organism that has an extremely active glycolytic cycle, which is a source of MG through a secondary reaction of triosephosphate isomerase (*5, 6*). Several studies suggest that the GSH-dependent glyoxalase enzyme system also deserves renewed interest as a potential target for antitumor drug development (*7, 8*).

Structurally, GlxI occur as homodimeric or fused dimer protein structures. Examples of homodimeric GlxI enzymes include those from *Escherichia coli* (*9*), humans (*10*), *Leishmania major* (*11*), and *Pseudomonas putida* (*12*). In most representative proteins of the $\beta\alpha\beta\beta\beta$ superfamily, which includes GlxI, the overall assembly of monomers results in the formation of two seemingly identical active sites/binding sites at the dimeric interface. However, fused dimeric GlxI enzymes have been isolated primarily from *Saccharomyces cerevisiae* (*13*), *P. falciparum* (*14*), and plant sources such as wheat bran (*15*). In a fused dimer, all $\beta\alpha\beta\beta\beta$ modules are joined via protein linkers to form both active sites within a contiguous stretch of polypeptide sequence (*2*). Several studies of monomeric GlxI enzymes have allowed for some exploration of differential kinetics of the two active sites in the native protein (*13, 14*). These data provided evidence for allosteric coupling of the active sites in monomeric *P. falciparum* GlxI despite the observation of distinct substrate binding affinities when comparing these sites (*14*).

The *E. coli* GlxI protein was the first non-Zn^{2+}-activated (i.e., Ni^{2+}- or Co^{2+}-activated but Zn^{2+} inactive) GlxI reported. It contains 135 amino acid residues, and its X-ray structure has been determined to 1.5 Å resolution (*9*). The three-dimensional structure of the enzyme is homodimeric with what appears to be two identical active sites (Figure 1c). Each active site contains two histidine and two glutamic acid residues that coordinate to the metal ion along with two water molecules so that the catalytic metal ion has hexacoordinate geometry. All of the X-ray structures for the Ni^{2+}-, Co^{2+}-, Zn^{2+}- and Cd^{2+}-bound *E. coli* GlxI indicate that both active sites are occupied by metal ions, although Zn^{2+}-bound *E. coli* GlxI is inactive. However, previous enzymological and biophysical investigations have documented half-of-the-sites

[†] This research was financially supported by NSERC.

* Corresponding author. Tel: 519-888-4567 × 35817. Fax: 519-746 0435. E-mail: jhonek@uwaterloo.ca.

[‡] These authors contributed equally to this work.

[1] Abbreviations: Gdn-HCl, guanidine hydrochloride; GlxI, glyoxalase I; GlxII, glyoxalase II; GSH, glutathione; HBVG, *S*-{2-[3-(hexyloxy)benzoyl]vinyl}glutathione; HSQC NMR, heteronuclear single quantum coherence nuclear magnetic resonance; ICP, inductively coupled plasma; ITC, isothermal titration calorimetry; MG, methylglyoxal; MOPS, 3-(*N*-morpholino)propanesulfonic acid; SDS−PAGE, sodium dodecyl sulfate−polyacrylamide gel electrophoresis.

10.1021/bi8013278 CCC: $40.75 © 2008 American Chemical Society
Published on Web 11/20/2008

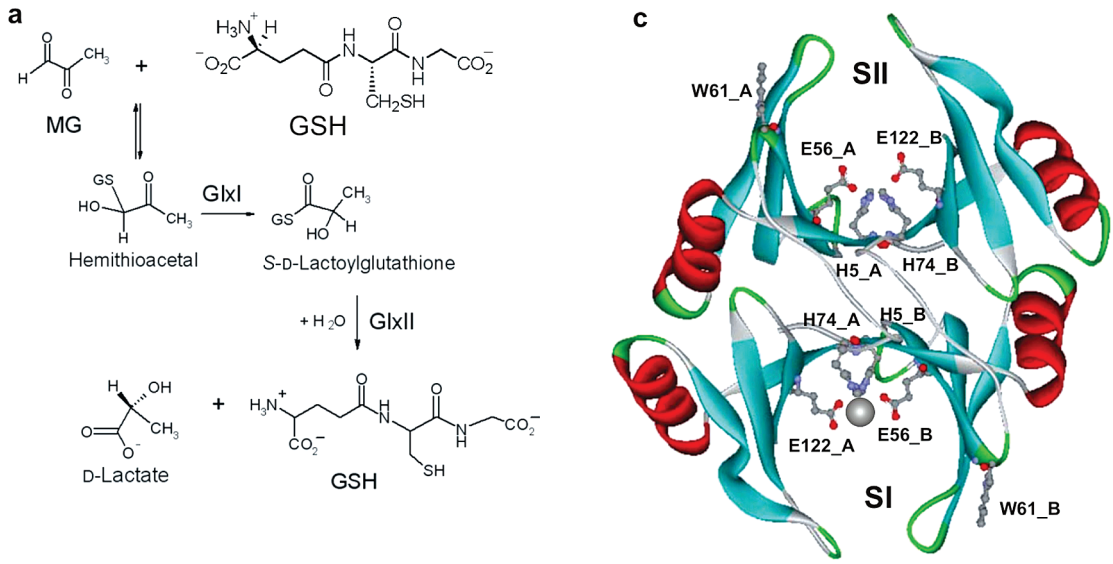

b

```
Chain_A: 10         20         30         40         50         60         70         80
MRLLHTMLRV GDLQRSIDFY TNVLGMKLLR TSENPEYKYS LAFVGYGPET EEAVIELTYN WGVDKYELGT AYGHIALSVD
         90         100        110        120        130
NAAEACEKIR QNGGNVTREA GPVKGGTTVI AFVEDPDGYK IELIEEKDAG RGLGN

Chain_B: 10         20         30         40         50         60         70         80
MRLLHTMLRV GDLQRSIDFY TNVLGMKLLR TSENPEYKYS LAFVGYGPET EEAVIELTYN WGVDKYELGT AYGHIALSVD
         90         100        110        120        130
NAAEACEKIR QNGGNVTREA GPVKGGTTVI AFVEDPDGYK IELIEEKDAG RGLGN
```

FIGURE 1: Two symmetrical active sites in *E. coli* GlxI. (a) GlxI is the first enzyme in the two component GlxI system. (b) Homodimeric *E. coli* GlxI consists of two identical polypeptide chains with one tryptophan on each chain at position 61. (c) Solid ribbon representations of the X-ray structures of *E. coli* GlxI shows two symmetrical active sites [PDB code: 1F9Z], where one metal ion has been observed in each individual active site. Amino acid residues coordinating the metal ion in the active sites are shown in stick format in the central, vertical cleft of the protein. Note that one metal ion has been removed from one of two active sites for clarity.

metallation in these two supposedly identical active sites in *E. coli* GlxI (*16, 17*). In order to evaluate whether these observations are related to protein conformational dynamics in each active site, we have utilized $^{15}N-^{1}H$ HSQC NMR titration experiments to monitor resonance perturbation during metal (Ni^{2+}) and inhibitor binding to the enzyme. The current results provide NMR evidence for half-of-the-sites Ni^{2+} binding in *E. coli* GlxI. Of particular interest is the observation that *E. coli* apo-GlxI possesses inherent asymmetry when comparing the monomeric modules.

EXPERIMENTAL PROCEDURES

Protein Expression and Purification. All cultures for overproduction of ^{15}N-labeled protein were grown on a 0.5 or 1 L scale. Wild type *E. coli* GlxI was overproduced in an *E. coli* BL21 (DE3) host with the plasmid pGL10, which contains the *E. coli* GlxI gene (*16*). Large-scale M9 cultures containing 50 mg·L^{-1} carbenicillin and 1 g·L^{-1} ^{15}N-labeled ammonium sulfate (sole nitrogen source) were inoculated with growth from a 20 mL M9 culture (containing unlabeled $(NH_4)_2SO_4$ as a nitrogen source) containing 50 μg·mL^{-1} carbenicillin. The intermediate M9 culture was initially inoculated with growth from a 10 mL LB starter culture containing 50 μg·mL^{-1} carbenicillin. Prior to inoculating the intermediate and large-scale cultures, the inoculum was centrifuged at 3,000 × *g* and resuspended in fresh M9 salts solution to minimize the carry over of any secreted β-lactamase. The culture was grown to an OD_{600} of 1.0 and then induced with 0.5 mM IPTG for 12 h. Cells were harvested by centrifugation at 6000 × *g* and frozen in liquid nitrogen for storage at −80 °C.

For overproduction of the active site variant of *E. coli* GlxI, i.e., H74Q, *E. coli* MG1655 host strain containing the plasmid pGL13 was used (*18*). The protocol described above for the overproduction of wild type ^{15}N-labeled *E. coli* GlxI was similarly employed for labeling GlxI mutants.

Purification of wild-type GlxI involved precipitating contaminating proteins in the lysate (cells initially suspended in 20 mM Tris at pH 8.0) by the addition of $(NH_4)_2SO_4$ to 60% saturation. The majority of recombinant GlxI remains in the supernatant at this salt concentration, and this remaining soluble portion of the lysates was dialyzed into 20 mM Tris at pH 8.0 containing 1 mM PMSF for application to a Unosphere-Q anion exchange column (Biorad, Hercules, CA). The dialyzed protein was applied to the column (loaded at 0.8 mL·min^{-1}) and eluted using a linear gradient of KCl from 0 to 1 M over 100 min at 0.8 mL·min^{-1}. The GlxI fractions were eluted between 20 and 40% KCl and pooled for dialysis into 20 mM Tris at pH 8.5 and loaded onto a MonoQ 5/5 column at 0.5 mL·min^{-1}. The GlxI was eluted from the column with a linear gradient of KCl from 0 to 1 M over 100 min at 0.5 mL·min^{-1}. Fractions containing GlxI were pooled and concentrated using a Vivaspin 10 centrifugal concentrator (10,000 MWCO, Sartorius, Gottingen, Germany), followed by buffer-exchange. The protein was initially exchanged into 50 mM MOPS containing 100 mM 2,6-pyridinedicarboxylic acid (DPA) (pH 7.0) to ensure the removal of any bound metal as determined by metal ion analysis. Then the solution was exchanged into 20 mM MOPS (pH 6.6). The sample was quantitated by the method of Bradford, and the absence of any contaminating

metal was confirmed by the PAR (4-(2-pyridylazo)resorcinol) assay using protein denatured in 4 M Gdn-HCl (*19, 20*).

For the purification of ^{15}N-labeled mutant GlxI (i.e., H74Q), the lysate was subjected to ammonium sulfate precipitation as described for the wild type enzyme. It was found, however, that a significant quantity of mutant GlxI remained in the pellet following the addition of $(NH_4)_2SO_4$ to 60% saturation in the lysate. This protein was solubilized and desalted by dialysis into 20 mM Tris-HCl (pH 8.5) for application to a Unosphere-Q column where the protein was eluted using a linear gradient of KCl from 0 to 1 M over 100 min with a flow rate of 0.8 mL·min^{-1}. The fractions containing GlxI from this step were dialyzed into 20 mM Tris-HCl (pH 7.5), and solid $(NH_4)_2SO_4$ was added to the sample for a final concentration of 1 M. The sample was applied to a Phenyl HP Hi Sub (Amersham Biosciences) column with 20 mM Tris at pH 7.5 containing 1 M $(NH_4)_2SO_4$ at 1 mL·min^{-1} and eluted from the column with a linear decreasing gradient of $(NH_4)_2SO_4$ (1 to 0 M over 15 min). A polishing step using a size exclusion column was included when necessary during purification. Specifically, the concentrated mutant GlxI sample was applied to and eluted from a Superdex 75 10/30 column (Amersham Biosciences, Uppsala, Sweden) at 0.5 mL·min^{-1} using 20 mM Tris-HCl (pH 7.5) containing 150 mM $(NH_4)_2SO_4$. Subsequently, these fractions were pooled and the buffer exchanged and concentrated as described above for wild type GlxI.

^{15}N-labeled GlxI enzymes prepared for this investigation were >95% pure as assessed by SDS−PAGE with Coomassie Brilliant Blue staining. The averaged yields were approximately 1−2 mg of protein from 4 L of culture for both wild type and mutant *E. coli* GlxI under the described growth conditions.

NMR Measurements. All NMR spectra were collected at 25 °C on a Bruker Avance 600 or 700 MHz spectrometer equipped with a triple-resonance pulse-field gradient probe. ^{15}N−^{1}H HSQC NMR spectra (*21*) were recorded in the States-TPPI mode for quadrature detection (*22*). All of the NMR samples were prepared in the same buffer, (i.e., 50 mM sodium phosphate, 50 mM NaCl, and 95% H_2O/5% D_2O at pH 6.0.). ^{15}N−^{1}H HSQC titrations were performed by stepwise addition of Ni^{2+} or inhibitor (at a high concentration) into ^{15}N-labeled apo-wild type and H74Q *E. coli* GlxI enzymes (typically at a concentration of 0.1−0.3 mM) to a final 1- to 2-fold excess. For example, $NiCl_2$ stocks were prepared at concentrations such that the wild type dimeric enzyme was exposed to 0.25 equivalents of Ni^{2+} with the addition of 5 μL of metal chloride solution. Minimal changes in volume and pH were ensured throughout the sample preparations.

S-{2-[3-(Hexyloxy)benzoyl]vinyl}glutathione (HBVG, from Aldrich, UK) was solublized in 100% DMSO as a millimolar concentration working stock and titrated into the holoenzyme (Ni^{2+}-reconstituted) to minimize any detrimental effects of this organic solvent on the protein structure. Control NMR experiments containing the same amounts of DMSO alone with GlxI confirmed that no alteration of the enzyme's native structure resulted from the presence of this solvent.

Calculation of Dissociation Constants (K_d). The dissociation constants, K_d, for the binding of Ni^{2+} or HBVG to GlxI were determined by fitting the intensity change (in the case of Ni^{2+} binding) or the chemical shift data (in the case of inhibitor binding) of selected resonance peaks to a simple bimolecular association model as described by Lian et al. (*23*). Principally, the chemical shifts or the intensity changes are described as a function of ligand concentration so that the association between GlxI (P) and metal ion or inhibitor (L) can be described by the following equation

$$P + L \underset{k_{off}}{\overset{k_{on}}{\rightleftharpoons}} PL$$

The chemical shift change or intensity change (C) is related to the dissociation constant (K_d) as follows:

$$C = C_0 + (C_t - C_0) \times \left[\frac{K_d + L_T + P_T - \sqrt{(K_d + L_T + P_T)^2 - 4P_TL_T}}{2P_T}\right]$$

where C_0 and C_t are the chemical shifts or the intensities at the starting and end points of the titration, respectively. P_T is the total concentration of the apo-GlxI, and L_T is the total concentration of the ligand at any point in the titration. Fitting of the data was carried out using MicroCal (Northampton, MA) Origin 6.0.

RESULTS

NMR Characterization of E. coli GlxI. A uniformly ^{15}N-labeled *E. coli* GlxI was overproduced in *E. coli*, and the metal ions were completely removed by the chelator treatment described in the Experimental Procedures section for all of the initial NMR samples. Apo-GlxI was confirmed by colorimetric PAR assays, which have been used in other studies to detect metallated forms of GlxI (*19*). A ^{15}N−^{1}H-HSQC spectrum of the GlxI protein in apo-form was recorded at 25 °C (Figure 2a), and the spectrum displayed a good dispersion of resonance peaks. Theoretically, there should be 130 resonance peaks if the homodimer is symmetrical or there might be up to 260 resonance peaks as there are distinct resonances in one monomer compared to the other. In the spectrum, approximately 128 resonance peaks are observed, suggesting that the apo-form of the enzyme exists as either a symmetrical dimeric conformation or a monomer under the NMR solution conditions. However, size exclusion chromatography using a Superdex 75 column confirmed that the ^{15}N-labeled apo-GlxI is a homodimer like the unlabeled wild type enzyme (data not shown). As an exception to the resonances indicating dimer symmetry, two resonance peaks with similar intensity were observed for the indole ^{15}N−^{1}H resonances of tryptophan residues (i.e., at ∼ 10.6 ppm in the ^{1}H-axis). Examination of the GlxI amino acid sequence reveals that the monomer contains only one tryptophan residue at position 61 (i.e., W61 in Figure 1b). The appearance of two indole ^{15}N−^{1}H resonance peaks with similar intensity confirms that the apoprotein is in a homodimeric form in the NMR sample. In comparison with the intensity of these two resonances to the rest of the spectrum, it is unlikely that there exist two different populations of the same W61 residue in each monomer. Although we cannot exclude the possibility of the existence of conformational exchange over time for the same tryptophan residue, it is highly likely that there are two different conformations that exist for each tryptophan residue in the

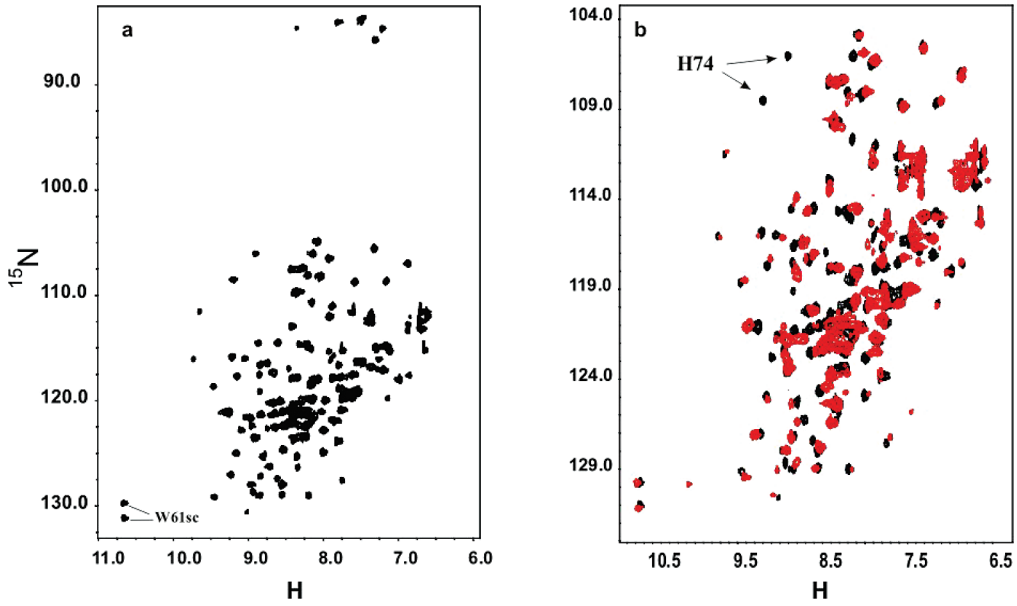

FIGURE 2: NMR Characterization of *E. coli* GlxI. (a) The $^{15}N-^{1}H$ HSQC spectrum of the wild-type apo-GlxI is well dispersed. $^{15}N-^{1}H$ resonance peaks of two W61 side-chains (labeled as W61sc) are separated and have identical intensities. (b) The HSQC spectrum of the GlxI H74Q (in red), an active default mutant, is superimposed on that of the wild-type apo-GlxI (in black). As a result, the resonance peaks for two H74 residues can be identified and are annotated as H74.

apoprotein so that the local conformations around two W61 residues are inherently asymmetric in the apoenzyme homodimer.

For simplification, the two active sites in GlxI were arbitrarily named SI (i.e., the active site at the bottom in Figure 1c) and SII (i.e., the active site at the top in Figure 1c). It should be noted that the two W61 residues are not equally positioned in the X-ray structure of homodimeric GlxI, and it would be of interest to determine whether there are any differences for metal ion binding residues between the two active sites. To quickly address this question, $^{15}N-^{1}H$ HSQC NMR analysis of an active site *E. coli* GlxI variant was performed. The variant H74Q GlxI has the native His74 metal ligand substituted with a Gln residue. The H74Q GlxI maintains a homodimeric quaternary structure in solution (Honek et al., unpublished data) as does the wild type enzyme (*24*). The overall distribution of ^{15}N -^{1}H HSQC resonance peaks for the H74Q GlxI is similar to those observed for the wild type enzyme (in red, Figure 2b). However, when these two spectra were superimposed, there were some notable differences between the HSQC spectrum of the H74Q mutant and that of wild type GlxI (Figure 2b). An obvious discrepancy observed is the absence of two peaks in the H74Q GlxI spectrum that are located at the points of (^{15}N 108.5 ppm, ^{1}H 9.25 ppm) and (^{15}N 106 ppm, ^{1}H 8.96 ppm) in the wild type GlxI spectrum. It is possible that H74 has two pairs of resonance peaks, and we arbitrarily assigned these two peaks to H74_A and H74_B, respectively, in each active site (Figure 2a). Their absence in the H74Q GlxI spectrum is plausible given the glutamine substitution at this position.

Furthermore, although we intended to assign the $^{15}N-^{1}H$ HSQC resonance peaks shown in Figure 2a utilizing $^{15}N/^{13}C$-labeled wild type GlxI, this goal was delayed for lack of sufficient quantities of double-labeled protein for NMR analysis, as the current protein expression system with plasmid pGL10 (see Experimental Procedures) was found to be greatly reduced in M9 media. Therefore, incorporation of a His-tag with six histidine residues and a thrombin cleavage sequence (i.e., L-V-P-R-G-S) into the C-terminus of the GlxI, to facilitate protein purification, was undertaken. Details of the construction of the new expression plasmid are described in Supporting Information. The new construct could overexpress His-tagged GlxI at the same efficiency as the original one, and the resulting protein could be readily purified using immobilized metal affinity chromatography on Ni-nitriloacetic acid (Ni-NTA) agarose beads. Eventually, sufficient quantities of the $^{15}N/^{13}C$-labeled protein containing the His-tag were prepared and used for NMR experiments to accomplish the NMR backbone assignment. The NMR protein sample exhibits a distribution of $^{15}N-^{1}H$ HSQC resonances (see Figure S1 in Supporting Information) very similar to the spectrum of non-His-tagged GlxI, although the new protein still contains four additional amino acid residues after the removal of the His-tag. A previous study observed that the removal of eight amino acid residues from the C-terminal of *E. coli* GlxI does not alter protein conformation and activity (*9, 16*). On the basis of the current work, the addition of four amino acid residues to the C-terminal of *E. coli* GlxI does not affect protein conformation. Through availability of the new GlxI NMR sample, assignment of 62% of the main-chain resonances using 3D HSQC-based NMR experiments was possible (Figure S1 in Supporting Information). Importantly, the assignment has not only confirmed the two different H74 resonances from the two individual active sites but also indicated that an amino acid segment, which includes T70, A71, Y72, G73, and H74, exhibits two distinct sets of resonances in the absence of metal ions (Figures S1 and S2 in Supporting Information). However, no double resonance peaks for the backbone were observed for other residues including W61, although the indole $^{15}N-^{1}H$ resonances of two W61 in dimeric GlxI are entirely different from each other. These data suggest the presence of distinct metal center environments in the *E. coli* GlxI dimer in the metal-free (apo) form.

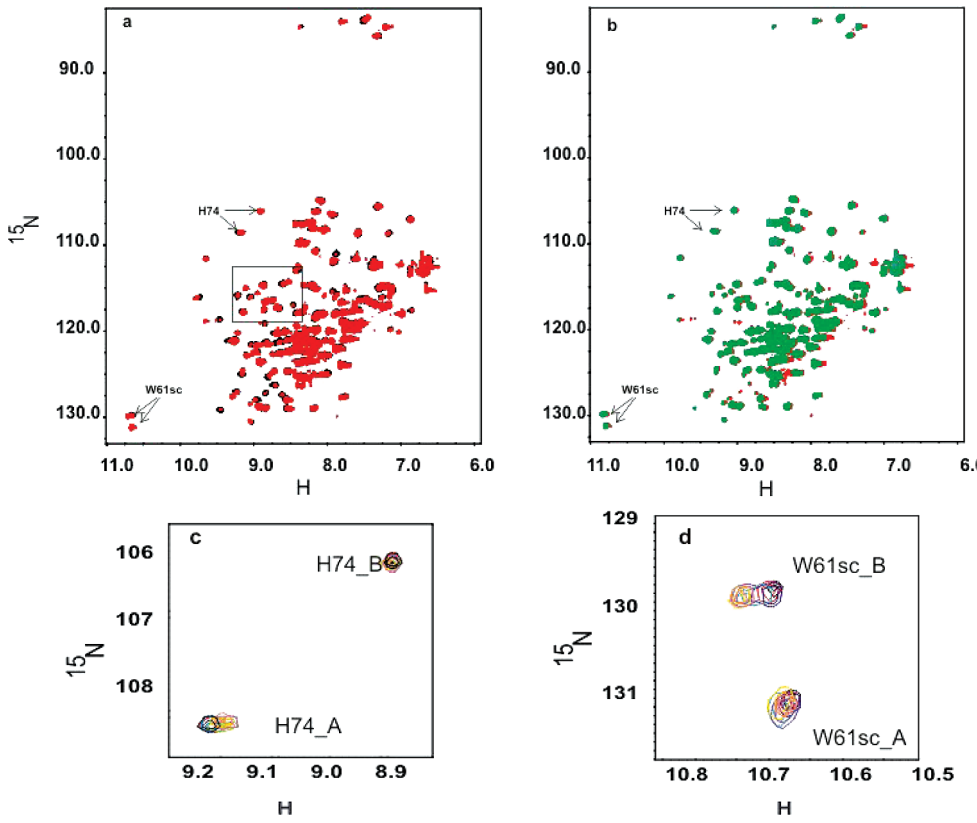

FIGURE 3: HSQC NMR titration of GlxI by Ni^{2+} ion. (a) The apo-GlxI (in black) was titrated with $NiCl_2$ to a ratio of 1:1 (dimer/metal ion), as shown in red. (b) The apo-GlxI was titrated with $NiCl_2$ to a ratio of 1:2 (dimer/metal ion) (in green), in comparison to that titrated with $NiCl_2$ to a ratio of 1:1 (in red). Two spectra are essentially similar to each other. (c) and (d) Chemical shifts for H74 and W61 side-chain $^{15}N-^{1}H$ resonances are depicted with Ni^{2+}-titration (dimer/metal) in a ratio of 1:0 (black), 1:0.4 (green), 1:0.6 (purple), 1:0.8 (yellow), 1:1 (red), 1:1.5 (brown), and 1:2 (blue). The illustration of these resonance peaks was simplified for clarity.

Another important attribute of the HSQC NMR spectrum obtained for the H74Q GlxI variant is that the two peaks associated with the indole ring, the $^{15}N-^{1}H$ resonances from W61, are still visible as observed in the wild type spectrum (Figure 2b). This implies that dimer asymmetry is present in the variant, which is plausible, as the histidine to glutamine substitution is not positioned to significantly alter the native structure of the enzyme (see Figure 1c).

Ni^{2+} Titration of the Apo-Form GlxI. In a second set of experiments, the incremental Ni^{2+}-titration of apo-GlxI was monitored by HSQC NMR to qualitatively assess subtle protein backbone reorganization associated with metal binding. These conformational changes are not detectable by X-ray or circular dichroism methods (*9, 17*). Following titration to one equivalent of Ni^{2+} ions in solution per GlxI dimer, the HSQC NMR spectra revealed a splitting pattern for several peaks indicating asymmetric metal binding (Figure 3a). Another seminal finding from the HSQC monitored Ni^{2+}-titration of apo-GlxI was that amide backbone repositioning was essentially complete after titration with one equivalent of Ni^{2+} into the apoenzyme sample. Superimposition of the 2D spectra following one-equivalent and two-equivalent additions of Ni^{2+} to *E. coli* GlxI revealed little alteration of the protein conformation when titrated past the molar equivalent to one-half of the total active sites in the sample (Figure 3b). Complete reconfiguration of the GlxI holoenzyme is achieved following the addition of one equivalent of Ni^{2+} and may be interpreted such that the active enzyme saturates metal binding at one equivalent Ni^{2+} per dimer. This data is completely consistent with previous isothermal titration calorimetry (ITC) and inductively coupled plasma-atomic emission spectroscopy (ICP-AES) studies as well as activity versus metal content plots indicating that *E. coli* GlxI exhibits half-of-the-sites metal binding under the conditions investigated (*16, 17*). Furthermore, only one of two H74 resonance peaks was affected during Ni^{2+} titration of the enzyme (i.e., H74_A), whereas another H74 resonance peak (i.e., H74_B) remained in a fairly constant position in the spectrum (Figure 3c). A similar phenomenon was also observed for the two W61 side-chains (i.e., W61sc in Figure 3d). We assigned the W61sc peak with significant chemical shift to the residue of W61sc_B (in SI site of Figure 1c), and it is close to the active site, which the H74_A residue locates in, and is directly involved with Ni^{2+} binding. As such, another W61sc $^{15}N-^{1}H$ resonance peak with insignificant chemical shift was assigned to W61sc_A in the SII site of the enzyme. As the chemical shifts of these peaks are a function of ligand concentration, the dissociation constants of Ni^{2+} with each active site, $K_{d,Ni}{}^{2+}$, based on H74_A and H74_B, can be calculated (see Experimental Procedures) as listed in Table 1.

Table 1: Dissociation Constants for Wild-Type GlxI Active Sites with Ni^{2+} Ion and HBVG

active site	resonance peak	$K_{d,\ Ni}{}^{2+}$ (μM)	$K_{d,\ HBVG}$ (μM)
SI	H74_A	0.065 ± 0.011	NSB
SII	H74_B	NSB[a]	364 ± 23.2

[a] NSB, no significant binding.

A selected region of the HSQC spectrum from Figure 3a is expanded and shown in Figure 4. It is notable that several

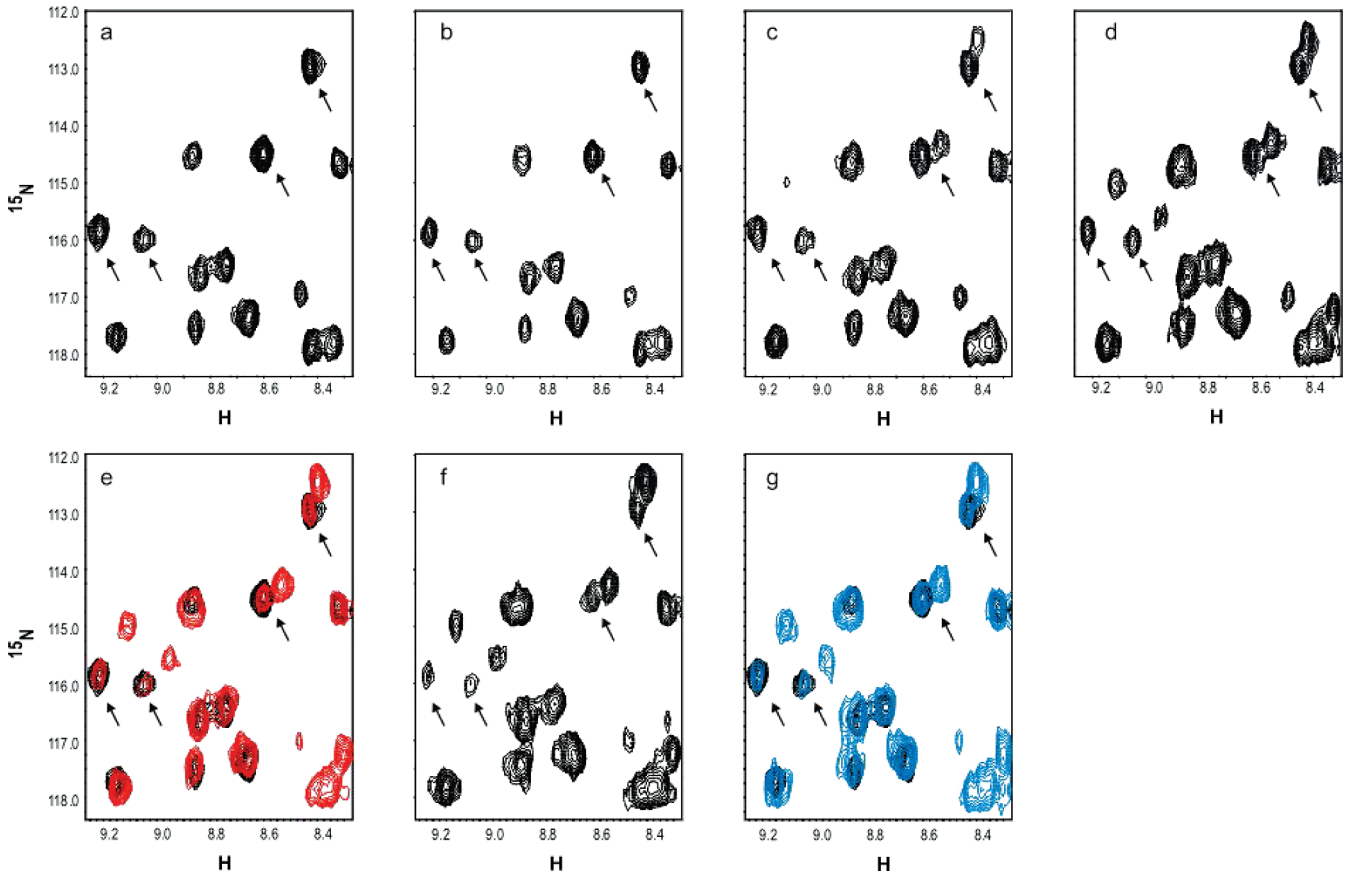

FIGURE 4: Splitting of resonance peaks during Ni^{2+} titration. A selected region of the HSQC spectrum of the apo-GlxI shows resonance perturbation when the Ni^{2+} concentration was altered from a ratio of 1:0 (dimer: metal) (a) to 1:0.25 (b), 1:0.5 (c), 1:0.75 (d), 1:1.5 (f), and 1:2 (g). Resonance peaks separated into two peaks are marked with arrows. In Panels e and g, the perturbed resonances, displayed in red (e) and in blue (g), respectively, are compared with the resonance peaks of the apo-GlxI in black (a).

resonance peaks (marked with arrows) are observed to split into two peaks of equal intensity when the apoenzyme (1:0 = dimer/metal ion) (Figure 4a) is titrated with Ni^{2+} to a ratio of 1:1 (Figure 4e) and to a ratio of 1:2 (Figure 4g). Spatially distinct shifts from their original apoenzyme positions were also observed (Figure 4a and 4b), which is indicative of uniform backbone reorganizations at specific locations in both monomers of the native enzyme.

In order to examine whether the Ni^{2+}-reconstituted GlxI can eventually form the protein/metal complexes in the ratio of 1:2 (one dimer/two metals), the Ni^{2+}-added NMR sample was placed at 4 °C, and its HSQC spectrum was measured biweekly. Three months later, it was found that those resonance peaks induced by Ni^{2+}-titration shifted entirely into new positions and appeared as sharper peaks, as shown in Figure 5a. The NMR sample was checked by mass spectrometry to confirm that the protein had not been degraded. In addition, we have excluded any possibility caused by aged $NiCl_2$ stock solution as $NiCl_2$ stocks of several weeks to months of age have been used to assay GlxI activity yielding specific activity values comparable to our previous values. Moreover, the oxidation state of nickel ion in solution likely remains as Ni^{2+} over this time period as higher oxidation states are usually found in obscure oxides and binary fluoride compounds (*25*). The new set of peaks was much sharper and more dispersed, although their intensities are much less than others, suggesting that a rigid conformation of GlxI/Ni^{2+} complexes may form during storage. These sharper peaks are different from those initially formed during Ni^{2+}-titration (Figure 5b). However, some resonance shifts initially observed during Ni^{2+}-titration appeared to move back to where they appeared at their original positions before Ni^{2+} titration in the spectrum of the apo-form, as compared in Figure 5c, in which the spectrum measured after storage is superimposed with the spectrum of the apo-form (in blue, Figure 2a).

However, PAR assays on this particular GlxI sample indicated that the aged enzyme is composed of one equivalent of Ni^{2+} per dimer, as shown in Figure S5 in Supporting Information. Activity assays revealed that the enzyme activity under the same conditions is not significantly affected.

Inhibitor Titration of Ni^{2+}-Saturated GlxI. Additional HSQC titration experiments were undertaken to examine whether each active site has a different affinity to substrate analogues in the absence of Ni^{2+} ions. A comparatively strong inhibitor, *S*-{2-[3-(hexyloxy)benzoyl]vinyl}glutathione (HBVG) (*24*), was one of several *S*-substituted glutathione analogues previously screened against *E. coli* GlxI for inhibitory activity. This compound has a micromolar inhibition constant for *E. coli* GlxI (~57 μM) (*24*). When HBVG was titrated into a freshly prepared apo-GlxI NMR sample in a ratio of 1:2 (one dimer/2 inhibitors), most of the HSQC peaks for the enzyme were altered in position (Figure 6a), indicating that there was a slow to medium conformational exchange. A very similar resonance perturbation was observed for the Ni^{2+} saturated GlxI NMR sample, which contained the Ni^{2+} ion in a ratio of 2:1 to protein dimer (data not shown).

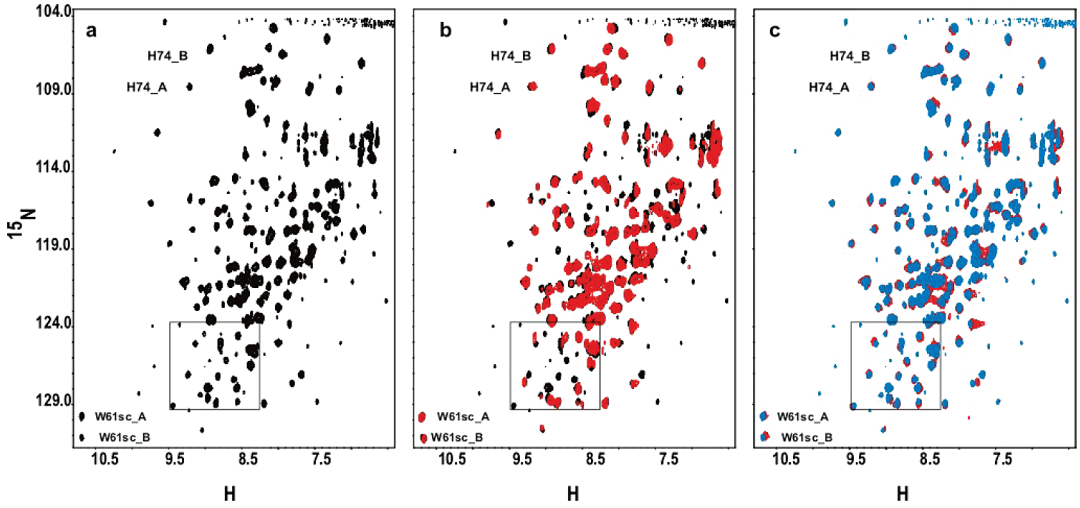

FIGURE 5: Observation of slow conformational exchange of *E. coli* GlxI with Ni^{2+} as evidenced by ^{15}N-^{1}H HSQC NMR. (a) The $^{15}N-^{1}H$ HSQC spectrum of GlxI in the presence of Ni^{2+} in a ratio of 1:2 (dimer/ion) was measured after the NMR sample was stored for three months at 4 °C. A region is highlighted in the box for comparison in panels b and c. (b) Comparison of the $^{15}N-^{1}H$ HSQC spectra of the Ni^{2+}-saturated GlxI is made between the freshly Ni^{2+}-titrated NMR sample (in red) and the same NMR sample hence after three months storage at 4 °C (in black, and is the same one shown in panel a). (c) Comparison of the $^{15}N-^{1}H$ HSQC spectra of the Ni^{2+}-saturated GlxI is made between the NMR sample after three months of storage at 4 °C (in red, and is the same one shown in panel a) and its original NMR sample of apo-GlxI (in blue, and is the same as that shown in Figure 2a).

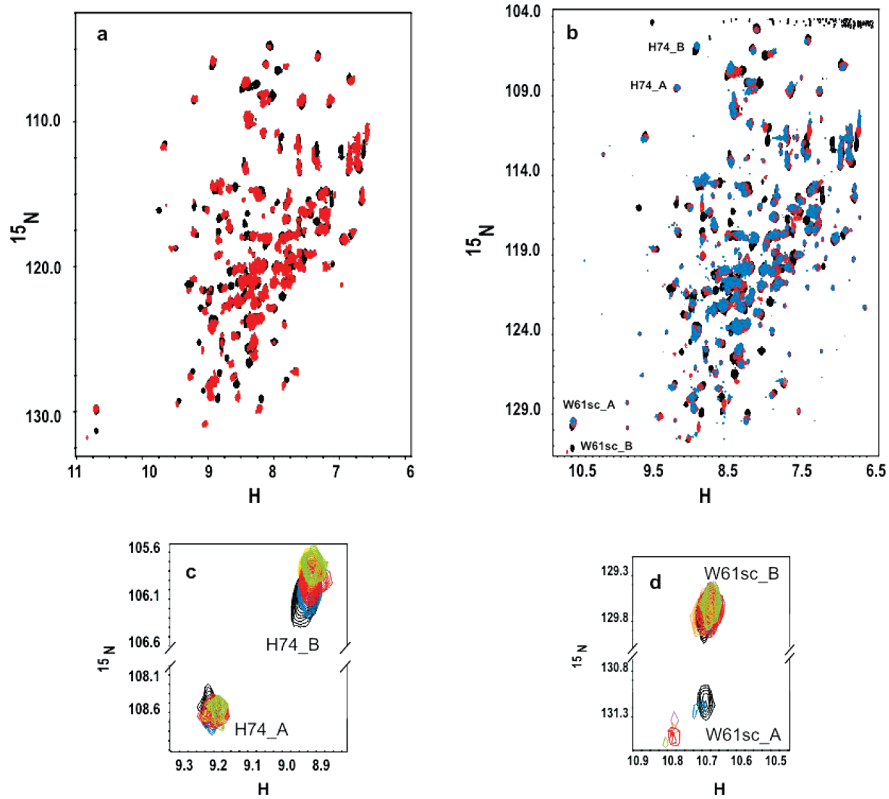

FIGURE 6: Titration of Ni^{2+}-saturated GlxI with inhibitor. (a) The apo-GlxI was titrated with HBVG to a ratio of 1:2 (dimer/inhibitor) (in red), as compared to the spectrum of apoenzyme in the absence of inhibitor (in black). (b) The Ni^{2+}-reconstituted GlxI (in black) was titrated with HBVG to a ratio of 1:1 (dimer/inhibitor) (in red) and to a ratio of 1:2 (in blue). (c) and (d) The $^{15}N-^{1}H$ resonance perturbations of H74 and W61 side-chain were measured when the inhibitor was titrated from a ratio of 1:0 (Ni^{2+}-saturated dimer/inhibitor) (black), 1:0.5 (blue), 1:1 (red) to a ratio of 1:2 (green). Illustration of W61sc_A resonances was simplified for clarity.

As the aged NMR sample contains different forms of the Ni^{2+}/dimer complexes (Figure 5), it was interesting to determine whether these complexes would respond differently to inhibitor binding. Figure 6b presents $^{15}N-^{1}H$ HQSC NMR resonance perturbation of the aged NMR sample by HBVG titration. While most of the resonance peaks were observed to be perturbed, the resonance peaks, which relate to the complex exhibiting an entirely new set of sharper resonance peaks, exhibited no response to inhibitor titration.

It is noteworthy that during titration with the inhibitor, the HSQC peak of H74_B in the SII site (Figure 1c) was observed to shift significantly, whereas the HSQC peak of H74_A in the SI site (Figure 1c) remained almost stationary (Figure 6b). The perturbation trends for specific peaks were

opposite to the initial Ni^{2+}-titration studies (see Figure 6). Interestingly, the two W61 indole $^{15}N-^{1}H$ resonance peaks were observed to be affected in a similar manner with response to inhibitor titration (Figure 6).

DISCUSSION

The current work presents convincing NMR evidence in favor of half-of-the-sites binding of metal ion (Ni^{2+}) in *E. coli* GlxI. These data differ from the *E. coli* GlxI X-ray data obtained on crystals of the protein, where each active site of the homodimer is occupied with a metal ion, as observed for the Ni^{2+}, Cd^{2+}, Co^{2+}, and Zn^{2+} holoforms. Our data are, however, consistent with isothermal titration calorimtery and metal activation studies (*16, 17*) and with evidence on the fused dimeric GlxI from *P. falciparum* where two active sites have different binding affinity for substrate (*14*).

The 2D HSQC spectrum of apo-GlxI revealed initial asymmetry of the monomeric modules comprising the native protein. This asymmetry is substantiated by the presence of nonequivalent resonance dispersion for one of the active site residues (e.g., H74) as well as one of the residues in close proximity to the active sites (e.g., W61). A key implication of the current results is that the nonuniform dimer environment likely plays a direct role in modulating the affinities of individual active sites for metal ions as well as substrate analogues.

Although nickel is a paramagnetic metal, we did not see any significant paramagnetic effects of Ni^{2+} on the HSQC NMR resonances during titrations within the Ni^{2+} concentration of <1 mM in this study, as described previously in other protein systems (*26*). Overall, during Ni^{2+} titration the backbone resonances from the $^{15}N-^{1}H$ HSQC spectra of the *E. coli* GlxI do not change dramatically so that major domain motions do not appear to accompany metal binding in this system. Rather subtle reorientations of small, discrete regions in the protein most likely accommodate Ni^{2+} binding based on the experimental data presented. This is in keeping with the absence of gross structural rearrangements accompanying the *E. coli* GlxI apo- to holoenzyme transition when analyzed by X-ray diffraction or by circular dichroism spectroscopy (*9, 17*). However, the preservation of overall enzyme structure is still subject to microscopic reconfigurations within the framework that is essential to metal recruitment in this particular GlxI. Resonance perturbation of the H74 residue in each active site by Ni^{2+}-titration is significantly different when the two sites are compared. This biased reconfiguration is mirrored in the chemical shift changes for W61 in response to metal ion binding (Figure 1c). Two residues (i.e., H74_A and W61_B) are likely located at the same active site and are significantly affected during metal titration. This implies that the active site containing these particular residues (e.g., SI site in Figure 1c) has much higher affinity than the other to Ni^{2+}-binding. This structural information confirms our previous enzymological and metal analysis data that strongly reflected a propensity toward nonequivalent metal binding in *E. coli* GlxI (*17*). However, *E. coli* GlxI is by no means the only metalloprotein in the biochemical literature for which half-of-the-sites metal binding is relevant to the active holoform of a matalloenzyme. The paradigm for half-of-the-sites metal binding has been carefully investigated in studies of the porphobilinogen synthase enzymes (*27, 28*), particularly that of *Drosophila melanogaster* porphobilinogen synthase (*29*). Recently a comparative study of symmetrical active sites in *P. falciparum* GlxI has provided insight into the microscopic properties of catalytic centers in fused GlxI enzymes (*14*). *P. falciparum* GlxI is a Zn^{2+}-activated GlxI enzyme that exhibits biphasic kinetics (*14*). These kinetic data were the basis for the authors' investigation of differential activity and allosteric coupling between the two catalytic sites in this protein. Although the structure of *P. falciparum* GlxI is currently not available, our structural evidence on the nonequivalence of two active sites in *E. coli* GlxI should provide a basis for evaluating the similarity of active sites in GlxI enzymes.

During the NMR titration experiments, we observed many asymmetrical residues for the apo-form of this homodimer (see Figure 4). Some resonance peaks were split into separate resonances upon Ni^{2+} saturation, suggesting that the local conformations surrounding these residues are symmetrical in the homodimer of the apo-GlxI, and become asymmetric with metal binding in the enzyme. These results further confirm that the nonequivalent binding of Ni^{2+} is mainly determined by intrinsic asymmetric conformation between the two active sites.

We also observed that the Ni^{2+}-titrated GlxI undergoes a slow conformational exchange after Ni^{2+}-titration and forms a new Ni^{2+}/dimer complex. This exchange was slow (requiring several weeks) and yielded a markedly different profile of HSQC spectrum for the wild type enzyme (see Figure 5a). This new set of resonance peaks was not due to the degraded enzyme, as mass spectrometry provided no indication of a significant population of degradative peptide fragments (data not shown). The appearance of the new set of sharp resonance peaks indicates that a rigid protein conformation formed. This complex may contain two Ni^{2+} ions per dimer, with Ni^{2+}-bound in each individual active site, a structure entirely consistent with previous X-ray structural investigations. However, a new protocol with higher sensitivity will be required to determine the presence of the second Ni^{2+} in this form of GlxI. Regardless, the biological activity of GlxI is not altered during storage mixed with the Ni^{2+} ion. Nevertheless, it is interesting to find that this new complex is not sensitive to inhibitor binding (see below).

It is likely that the particular inhibitor (i.e., HVBG) used in the current study has a different selectivity for the active sites of GlxI, compared to that of Ni^{2+} ions. Nevertheless, the current finding supports previous mass spectrometric and enzyme kinetic studies, indicating that GlxI can bind the HBVG in the apo- and Ni^{2+}-reconstituted forms (*24*). Given that several lines of experimental data now indicate monometallation of the *E. coli* holoenzyme (ITC, ICP-AES, and now HSQC NMR) (*17*), both apo- and holo-active sites of *E. coli* GlxI appear to be capable of binding substrate analogues. The extrapolation that these different active sites may also be catalytically active is intriguing, but it may also imply that a potential mode of *E. coli* GlxI inhibition is the presence of a compound that binds indiscriminately to both active sites, catalytic and noncatalytic. Further biochemical assays and detailed NMR structural studies of the Ni^{2+}/HBVG/GlxI complexes are required to solve these uncertainties.

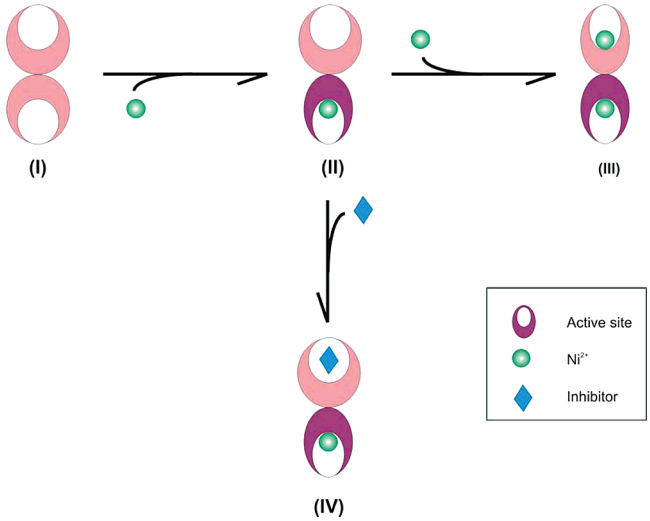

FIGURE 7: A putative mechanism for the metalation and inhibitor-binding of *E. coli* GlxI. Apo-GlxI has an intrinsic asymmetric local conformation for two symmetric active sites (I) so that only one active site in its apo-form can initially bind to one Ni^{2+} ion, forming a relatively stable intermediate complex (II), as evidenced by $^{15}N-^{1}H$ HSQC NMR titration (Figure 3a). This complex could slowly bind to one more Ni^{2+} ion, resulting in a more rigid conformation, which is not active for inhibitor binding (III). However, the half-site of Ni^{2+}-bound *E. coli GlxI* has high affinity for an inhibitor (i.e., HBVG) in the active site without Ni^{2+}-bound (IV), although the Ni^{2+}-bound active site has weak affinity for this inhibitor.

Taken together, the titration of the *E. coli* apo-GlxI enzyme with Ni^{2+} indicates that Ni^{2+} only metallates one of two seemingly identical active sites in this dimeric enzyme, resulting in reorganization of the enzyme conformation for metal or inhibitor binding at the other active site of the dimer (Figure 7). Therefore, the current results provide a new mechanism for understanding metal binding in *E. coli* GlxI and for the potential design of new inhibitors of GlxI. To completely understand the origin of asymmetry in this enzyme, detailed NMR structures of the apo-GlxI and the Ni^{2+}-/HBVG/GlxI complexes will be required.

ACKNOWLEDGMENT

We thank Dr. Elisabeth Daub for her valuable discussions and Valerie Robertson (University of Guelph), Janet Venne, Dr. Richard Smith, and Dr. Michael Ditty for their technical assistance. We wish to thank the referees of our manuscript for their helpful suggestions and comments.

SUPPORTING INFORMATION AVAILABLE

Molecular cloning, overexpression, and purification of $^{15}N/^{13}C$-labeled His-tagged *E. coli* GlxI; assignment of backbone ^{N}H, ^{15}N, $^{13}C^{\alpha}$, and $^{13}C^{\beta}$, and biochemical assays on the metal stoichoimetry and activity of GlxI over aging process. This material is available free of charge via the Internet at http://pubs.acs.org.

REFERENCES

1. Sukdeo, N., Daub, E., and Honek, J. F. (2007) Biochemistry of the Nickel-Dependent Glyoxalase I Enzymes, in *Nickel and Its Surprising Impact in Nature* (Sigel, A., Sigel, H., and Sigel, R.K.O., Eds.) pp 445−471, John Wiley & Sons, Ltd,, New York.
2. Thornalley, P. J. (2003) Glyoxalase I--structure, function and a critical role in the enzymatic defence against glycation. *Biochem. Soc. Trans. 31*, 1343–1348.
3. Creighton, D. J., and Hamilton, D. S. (2001) Brief history of glyoxalase I and what we have learned about metal ion-dependent, enzyme-catalyzed isomerizations. *Arch. Biochem. Biophys. 387*, 1–10.
4. Rae, C., Berners-Price, S. J., Bulliman, B. T., and Kuchel, P. W. (1990) Kinetic analysis of the human erythrocyte glyoxalase system using 1H NMR and a computer model. *Eur. J. Biochem. 193*, 83–90.
5. Allen, R. E., Lo, T. W., and Thornalley, P. J. (1993) Inhibitors of glyoxalase I: design, synthesis, inhibitory characteristics and biological evaluation. *Biochem. Soc. Trans. 21*, 535–540.
6. Barnard, J. F., Vander Jagt, D. L., and Honek, J. F. (1994) Small molecule probes of glyoxalase I and glyoxalase II. *Biochim. Biophys. Acta 1208*, 127–135.
7. Creighton, D. J., Zheng, Z. B., Holewinski, R., Hamilton, D. S., and Eiseman, J. L. (2003) Glyoxalase I inhibitors in cancer chemotherapy. *Biochem. Soc. Trans. 31*, 1378–1382.
8. Antognelli, C., Baldracchini, F., Talesa, V. N., Costantini, E., Zucchi, A., and Mearini, E. (2006) Overexpression of glyoxalase system enzymes in human kidney tumor. *Cancer J. 12*, 222–228.
9. He, M. M., Clugston, S. L., Honek, J. F., and Matthews, B. W. (2000) Determination of the structure of *Escherichia coli* glyoxalase I suggests a structural basis for differential metal activation. *Biochemistry 39*, 8719–8727.
10. Cameron, A. D., Olin, B., Ridderstrom, M., Mannervik, B., and Jones, T. A. (1997) Crystal structure of human glyoxalase I: evidence for gene duplication and 3D domain swapping. *EMBO J. 16*, 3386–3395.
11. Ariza, A., Vickers, T. J., Greig, N., Armour, K. A., Dixon, M. J., Eggleston, I. M., Fairlamb, A. H., and Bond, C. S. (2006) Specificity of the trypanothione-dependent *Leishmania major* glyoxalase I: structure and biochemical comparison with the human enzyme. *Mol. Microbiol. 59*, 1239–1248.
12. Saint-Jean, A. P., Phillips, K. R., Creighton, D. J., and Stone, M. J. (1998) Active monomeric and dimeric forms of *Pseudomonas putida* glyoxalase I: evidence for 3D domain swapping. *Biochemistry 37*, 10345–10353.
13. Frickel, E. M., Jemth, P., Widersten, M., and Mannervik, B. (2001) Yeast glyoxalase I is a monomeric enzyme with two active sites. *J. Biol. Chem. 276*, 1845–1849.
14. Deponte, M., Sturm, N., Mittler, S., Harner, M., Mack, H., and Becker, K. (2007) Allosteric coupling of two different functional active sites in monomeric *Plasmodium falciparum* glyoxalase I. *J. Biol. Chem. 282*, 28419–28430.
15. Johansen, K. S., Svendsen, I. I., and Rasmussen, S. K. (2000) Purification and cloning of the two domain glyoxalase I from wheat bran. *Plant Sci. 155*, 11–20.
16. Clugston, S. L., Barnard, J. F., Kinach, R., Miedema, D., Ruman, R., Daub, E., and Honek, J. F. (1998) Overproduction and characterization of a dimeric non-zinc glyoxalase I from *Escherichia coli*: evidence for optimal activation by nickel ions. *Biochemistry 37*, 8754–8763.
17. Clugston, S. L., Yajima, R., and Honek, J. F. (2004) Investigation of metal binding and activation of *Escherichia coli* glyoxalase I: kinetic, thermodynamic and mutagenesis studies. *Biochem. J. 377*, 309–316.
18. Sukdeo, N. (2003) Comparative biochemistry and mutagenesis of bacterial glyoxalase I enzymes, M.S. Thesis, University of Waterloo, Waterloo, Canada.
19. Sukdeo, N., and Honek, J. F. (2007) *Pseudomonas aeruginosa* contains multiple glyoxalase I-encoding genes from both metal activation classes. *Biochim. Biophys. Acta 1774*, 756–763.
20. O'Young, J., Sukdeo, N., and Honek, J. F. (2007) *Escherichia coli* glyoxalase II is a binuclear zinc-dependent metalloenzyme. *Arch. Biochem. Biophys. 459*, 20–26.
21. Bodenhausen, G., and Ruben, D. J. (1980) Natural abundance nitrogen-15 NMR by enhanced heteronuclear spectroscopy. *Chem. Phys. Lett. 69*, 185–189.
22. States, D. J., Haberkorn, R. A., and Ruben, D. J. (1982) A two-dimensional nuclear overhauser experiment with pure absorption phase in four quadrants. *J. Magn. Reson. 48*, 286–292.
23. Lian, L. Y., Barsukov, I. L., Sutcliffe, M. J., Sze, K. H., and Roberts, G. C. (1994) Protein-ligand interactions: exchange processes and determination of ligand conformation and protein-ligand contacts. *Methods Enzymol. 239*, 657–700.
24. Stokvis, E., Clugston, S. L., Honek, J. F., and Heck, A. J. (2000) Characterization of glyoxalase I (*E. coli*)-inhibitor interactions by

electrospray time-of-flight mass spectrometry and enzyme kinetic analysis. *J. Protein Chem. 19*, 389–397.
25. Mackkay, R. A. and Henderson, W. (2002) *Introduction to Modern Inorganic Chemistry*, CRC Press, Boca Raton, FL.
26. Bertini, I., Luchinat, C., Parigi, G., and Pierattelli, R. (2008) Perspectives in paramagnetic NMR of metalloproteins. *Dalton Trans.* 3782–3790.
27. Jaffe, E. K. (1995) Porphobilinogen synthase, the first source of heme's asymmetry. *J. Bioenerg. Biomembr. 27*, 169–179.
28. Jaffe, E. K. (2005) Morpheeins: a new structural paradigm for allosteric regulation. *Trends Biochem. Sci. 30*, 490–497.
29. Kundrat, L., Martins, J., Stith, L., Dunbrack, R. L., Jr., and Jaffe, E. K. (2003) A structural basis for half-of-the-sites metal binding revealed in *Drosophila melanogaster* porphobilinogen synthase. *J. Biol. Chem. 278*, 31325–31330.

BI8013278